OVERVIEW OF TOKAMAK RESULTS

Bernhard Unterberg and Ulrich Samm
Institut für Plasmaphysik, Forschungszentrum Jülich GmbH*, Association EURATOM-FZ Jülich
D-52425 Jülich, Germany, phone: +49 2461 61 4803, email: B.Unterberg@fz-juelich.de

ABSTRACT

An overview is given of recent results obtained in tokamak devices. We introduce basic confinement scenarios as L-mode, H-mode and plasmas with an internal transport barrier and discuss methods for profile control. Important findings in DT- experiments at JET as α- particle heating are described. Methods for power exhaust like plasma regimes with a radiating mantle and radiative divertor scenarios are discussed. The overall impact of plasma edge conditions on the general plasma performance in tokamaks is illustrated by describing the impact of wall conditions on confinement and the edge operational diagram of H-mode plasmas.

I. INTRODUCTION

The tokamak has emerged as the leading concept to confine high temperature plasmas [1] (cf. also [2] for an overview of experimental results from Tokamaks). The progress of this research can be illustrated by the fusion product $n_{DT}\tau_E T_i$, which represents a figure of merit for plasma performance and which could be increased by several orders of magnitude (Fig. 1) during four decades of research on magnetic confinement. Most of this progress is based on building successively larger devices rather than on improvements of the thermal insulation (energy confinement) caused by the magnetic field. The largest and most powerful tokamak devices, JET and JT-60U, have reached plasma parameters (only D-fuelling) equivalent to "break even" ($Q = P_{fus}/P_{aux} = 1$) [3] [4]. With DT-fuelling in JET and TFTR hot plasmas producing a fusion power of up to 16.1 MW [5] and 10.7 MW [6] have been obtained.

The experience gathered so far has now resulted in the design of a next step device (ITER [8]) to achieve a significant fusion gain of $Q = 10$. This device will provide the necessary physics and engineering information for the development of a demonstration tokamak power plant (DEMO). The site of ITER is now decided to be located in Cadarache, France. Meanwhile, different types of plasma regimes are foreseen for this device [9].

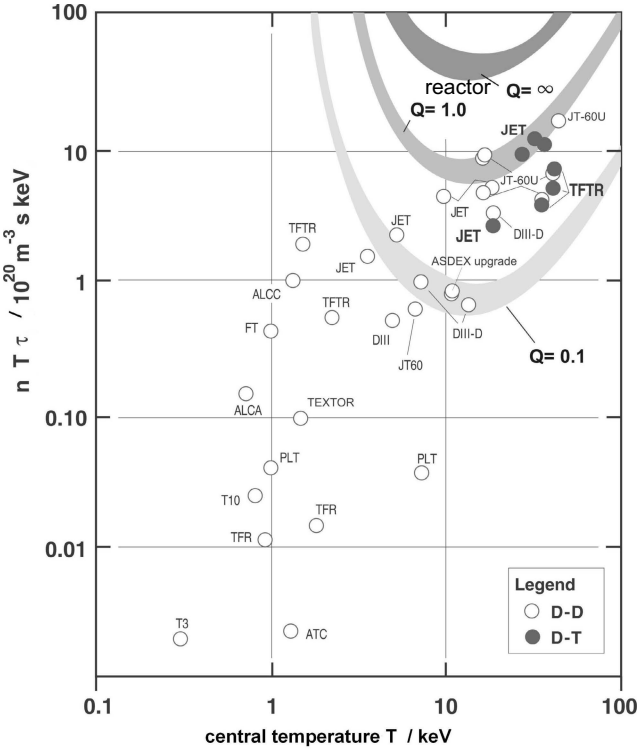

Figure 1: Fusion triple product (adapted from [6] including results presented in [4] [7])

The first base-line regime in inductive operation is the ELMy H-mode, an improved confinement regime with a transport barrier at the edge, where periodic bursts of particle and energy flow ("edge localized modes") ensure quasi- stationary operation without impurity or helium ash accumulation. The extrapolation of this regime to the next step is based on empirical scalings obtained from a multi-machine data base. These projections satisfy the constrains to describe the energy confinement time in terms of dimensionless physics parameters ("wind tunnel approach" [10] [11]).

Alternative confinement regimes have been found in recent years and are now subject to detailed investigations. Most interesting are those which rely on non-inductive current drive resulting in reversed (negative) or flat magnetic shear profiles. The magnetic shear is the change of the helical twist of field lines with the mi-

*Partner in the Trilateral Euregio Cluster

nor radius defined as $S = (r/q)(dq/dr)$ where q is the safety factor. Internal transport barriers are created in the plasma core leading to substantially improved confinement (2-3 times higher than in ELMy H-mode discharges) and improved stability (increased normalized pressure β_N). These so called "advanced tokamak concepts" open the prospect to both more compact and steady- state tokamak power plants [12] [13] [14]. Such a regime is envisaged as a second option for ITER to show steady- state operation at $Q = 5$ based on current drive and bootstrap current. Most recently a so-called "advanced" H-mode scenario has been developed in present devices [15] which combines attractive features of both regimes discussed before. All scenarios will be introduced in the next section.

However, stationary operation in a fusion device requires more than plasma current drive. The issues of helium exhaust, power exhaust and erosion from plasma facing components are of paramount importance for extended burn in a fusion plasma. All confinement scenarios envisaged have to be compatible with the constrains resulting from these issues. The plasma edge plays a two- fold role in this context: on the one hand the physical processes in the edge determine exhaust and erosion properties, on the other hand they influence the global plasma performance in a crucial way.

II. TOKAMAK CONFINEMENT SCENARIOS AND PROFILE CONTROL

Since the early days of tokamak research it has turned out that radial transport cannot be explained by Coulomb collisions in toroidal geometry (so called neoclassical theory). Instead "anomalous transport" has been found where turbulent processes of various kinds are responsible for enhanced transport. In recent years tremendous progress has been made to describe the turbulent transport theoretically (see e.g. [16]), in particular with the help of complex computer codes which calculate the growth rates of the underlying instabilities and allow to deduce the resulting transport coefficients (see e.g. [17] [18] [19] [20]).

However, so far none of these models describes anomalous transport properly in accordance with *all* the various experimental results over the whole plasma cross section. Therefore, experimental findings are still categorized according to their empirical signatures into confinement "modes" or "scenarios". Sudden transitions between such regimes are often observed. Fig. 2 illustrates qualitatively the characteristic temperature profiles of three of these regimes [5].

The *L-mode* ("low" confinement mode) is the most common mode of tokamak operation when auxiliary heating is applied. The inner part of the discharge is generally affected by periodic, crash like turbulent re-

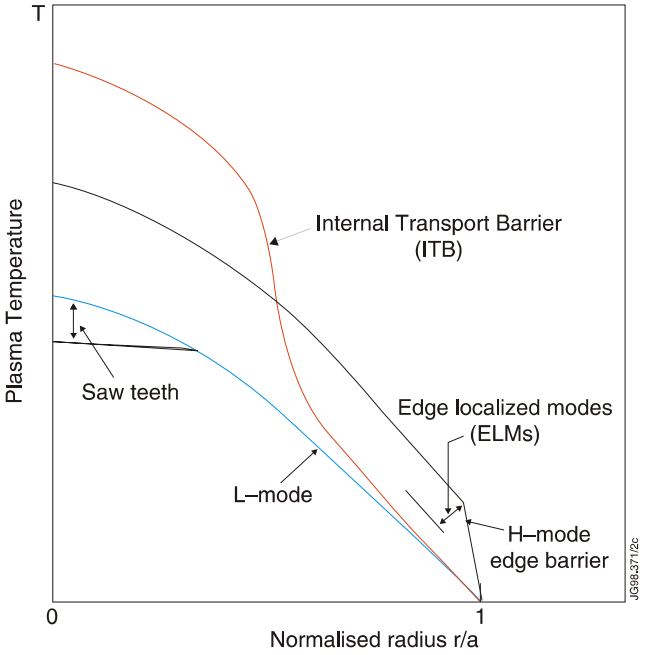

Figure 2: Tokamak temperature profiles for a number of modes of operation (adapted from [5])

arrangements of the temperature, density and current profiles ("sawtooth" crashes) connected with the formation of a helical m=1/n=1 mode [21] and the flattening of the profiles inside the q=1 surface. Although on average the sawtooth instability reduces the stored energy it is beneficial for expelling impurities which otherwise could accumulate in the plasma core. Active profile control by current drive [22] can be used to tailor the sawtooth frequency and its amplitude.

The *H-mode* ("high" confinement mode), which has first been observed in the divertor tokamak ASDEX [23] and later in other divertor and some limiter tokamaks, is characterized by an improvement of the energy confinement time by a factor of about 2 compared to the standard L-mode. Empirically it has been found that the transition to H-mode takes place above a certain threshold of the heating power. The H-mode is characterized by a transport barrier building up at the plasma edge with large gradients of the plasma pressure. Above a critical pressure gradient MHD instabilities develop leading to events called "edge localized modes" (ELMs), which reduce the edge pressure periodically by expelling energy and particles out of the plasma. While the H-mode is transient in nature without ELMs ("ELM-free H-mode") and characterized by an uncontrolled impurity accumulation, H-mode discharges with ELMs ("ELMy H-mode") can be maintained under quasi-steady state. Recently, regimes without ELMs have been found in a few devices where other MHD fluctuations in the edge lead to a particle

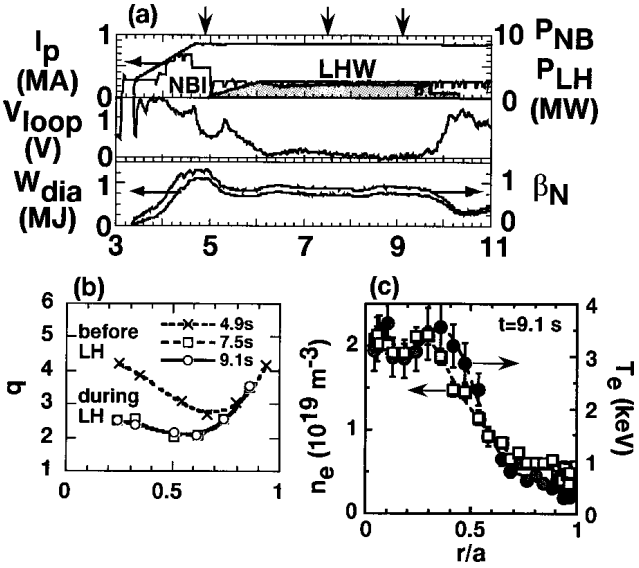

Figure 3: Reversed shear discharge in JT-60U [7]: a) plasma current I_p, neutral beam power P_{NBI}, lower hybrid power P_{LH}, surface loop voltage V_{loop}, diamagnetic energy W_{dia} and normalized beta β_N, b) radial profiles of safety factor before and during the application of the LH waves and c) electron density and temperature profiles

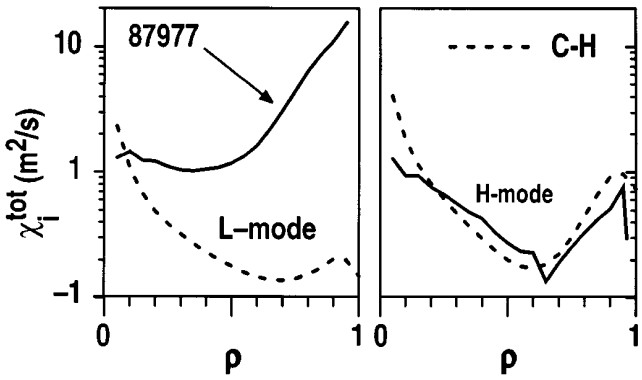

Figure 4: Ion thermal diffusivity vs ρ (square root of the normalized toroidal flux) in a negative central shear discharge in DIII-D [26]. The solid lines are the experiment, the dashed lines are the calculated neoclassical values. a) L-mode phase, b) H-mode phase

transport across the edge barrier sufficient to maintain stationarity ("Enhanced D_α mode" in Alcator C-mod [24], "Quiescent H-mode" in DIII-D [25]). So far, the ELMy H- mode is the first choice for the operating regime in the next step device. The quality of confinement in the H-mode is very much depending on the ELM frequency (confinement decreases with higher frequencies), and the height of the "edge pedestal" (i.e. temperature/ pressure at the top of the transport barrier). As a consequence, the plasma edge conditions influence strongly the global confinement as further described in section V.

Improved confinement can also be obtained by tailoring the current density profile to realize weak or negative magnetic shear (weakly hollow current density profiles) with $q > 1$ everywhere in the plasma. The stabilizing effect on both MHD and micro- turbulence driven instabilities can lead to *internal transport barriers* (ITBs) characterized by steep gradients of plasma profiles in the core. It became possible to optimize the magnetic shear profile by controlling the current diffusion during the current ramp-up phase of the discharge together with current drive by lower hybrid waves. The resulting current density profile may be aligned to the intrinsic bootstrap current in the tokamak (driven by the radial pressure gradient) with the potential of fully non- inductive and steady state plasma operation. An example of creating an internal transport barrier by active profile control in JT60-U is given in Fig. 3 [7]. In this discharge the plasma current is non- inductively driven (zero loop voltage!) with a bootstrap fraction of 23% while the remaining 77% is driven by lower hybrid waves. The reversed shear profile and the internal transport barrier seen at $r/a = 0.5$ could be maintained for 1.6 s. Fully non-inductive current drive has also been obtained with electron cyclotron waves in the tokamak TCV [28].

Best performance is obtained if an internal transport barrier is combined with a H-mode transport barrier at the edge. Under these conditions the confinement (of ions) can be close to neoclassical predictions over the whole minor plasma radius as shown in Fig. 4 [26] where the ion thermal diffusivity is depicted for the L-mode and the H-mode phase of a negative central shear discharge in DIII-D. The neoclassical ion diffusivity χ_i^{tot} has been calculated according to the formula of Chang-Hinton [27]. With a H-mode edge stability is improved with respect to ITB discharges with a L-mode edge owing to broader pressure profiles. Therefore, higher normalized plasma pressure β_N can be achieved in general ($\beta_N = 4$ for the discharge shown in Fig. 4). Recently, the combination of an internal transport barrier with a H-mode edge barrier could be shown under conditions where MHD oscillations at the edge instead of ELMs allow particle control (so called "quiescent double barrier H-mode" in DIII-D [29]). However, the operational domain of this regime is so far restricted to discharges with additional heating by neutral beams in direction opposite to the plasma current and to plasmas with low edge density [32] not favorable with respect to power exhaust in a future reactor.

Moreover, for the application of such a scenario in a fusion reactor it is important to investigate internal transport barriers under conditions where the electrons

are predominantly heated as it will be the case with heating by alpha particles. In ASDEX Upgrade internal transport barriers under conditions of $T_e \approx T_i$ could be achieved using electron cyclotron resonance heating [30]. ITB discharges are often found to suffer from impurity accumulation [31] [32], which can be attributed to neoclassical inward drifts driven by steep gradients of the fuel ion density. This is a serious problem to be solved.

Advanced H-mode scenarios could be a compromise and a very promising option for a future fusion reactor. Such modes of operation had been realized in all major tokamak devices as JET [33], DIII-D [34] and ASDEX-Upgrade [35]. A common feature is a very flat magnetic shear over a large central part of the plasma with $q_0 > 1$ everywhere. As a peculiarity, all of these scenarios have a mild MHD activity (e.g. in ASDEX-Upgrade so called fish bones, a m=1/n=1 oscillation in the very core of the discharge) which clamps the q- profile. As the safety factor in the plasma core is larger than 1 and sawtooth activity is therefore absent, these plasmas have in general no large neoclassical tearing modes [36] as a beta limiting instability. As a consequence, very high normalized plasma pressures at improved stability can be obtained.

III. DT- EXPERIMENTS

After the closure of TFTR, JET became the only tokamak worldwide capable of operating with a fuel mix of Deuterium and Tritium. In JET a maximum fusion power output of 16.1 MW has been obtained in an ELM-free hot ion H-mode with an edge confinement barrier in a DT- plasma and a resulting fraction Q of fusion power with respect to the total input power of 0.62 (trace I in Fig. 5). A quasi steady state ELMy H-mode discharge with plasma shape and safety factor q similar to that of ITER produced 4 MW fusion power for 5s corresponding to a total fusion energy of 22 MJ (trace III). An advanced tokamak regime using optimized magnetic shear configuration with an internal transport barrier has produced 8.2 MW (trace II).

The physics of alpha particles born in fusion reactions is one of the most important issues for DT experiments as the success of magnetic confinement reactors crucially depends on efficient alpha particle heating. Uncontrolled loss of alpha particles could diminish the heating power and furthermore lead to severe damage of plasma facing components. Alpha losses can occur as a consequence of first orbit losses of trapped alphas or imperfect axisymmetry (toroidal ripple losses). Furthermore, they can be caused by collective effects such as alpha particle induced instabilities (e.g. alpha driven fish bones and Alfén waves) which can be predicted as a function of the fast alpha velocity in relation to the

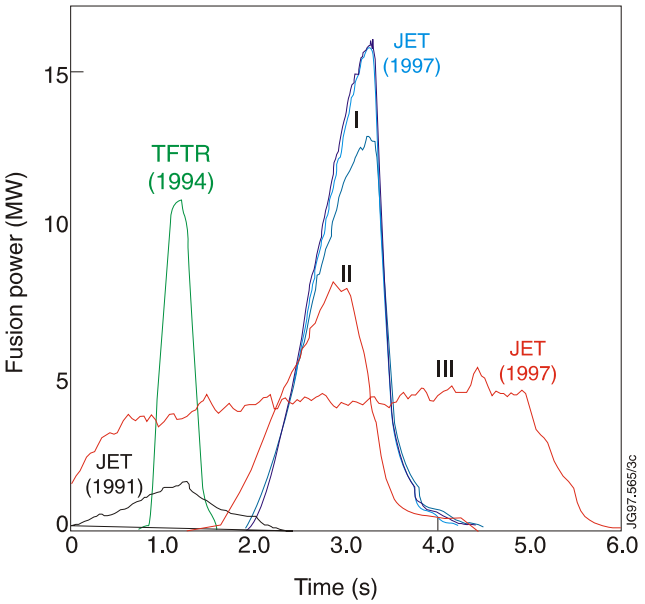

Figure 5: Fusion power development in the DT campaigns of JET and TFTR (adapted from [5])

Alfén velocity and the fast alpha pressure [37] [38]. The resulting confinement time of the fast alpha particles has to be compared to the time needed to thermalize with the background plasma as a result of Coulomb collisions (the classical slowing down time for alphas in a fusion plasma with $T_e = 15keV$ and $n_e = 10^{20}m^{-3}$ is about 0.7 s [39]). Present D-T experiments can already provide important conclusions on alpha particle physics as alpha particle density and pressure depend on the local plasma parameters and not on the fusion gain Q. It has turned out that alphas are well confined and slowing down is classical as concluded e.g. from the energy spectrum of alphas measured at TFTR and compared with code calculations [40].

Alpha particle heating has clearly been identified in D-T experiments in spite of the limited Q (Fig. 6). For this purpose at JET a DT- mixture scan has been performed with otherwise similar discharge parameters and with constant heating power by neutral beam injection ($P_{NBI} = 10.5MW$). A clear increase of the electron temperature is seen when the mixture approaches the optimum 50:50 ratio as expected.

IV. POWER AND PARTICLE EXHAUST

The duration of a burning fusion plasma will depend largely on the physics of the plasma at the boundary and in contact with the wall elements. The first wall has to withstand and exhaust the α- particle heating power and the helium ash must be removed (pumped) from the plasma. Wall erosion will affect the lifetime of wall elements and impurities are released into the plasma, which then cause fuel dilution and power loss

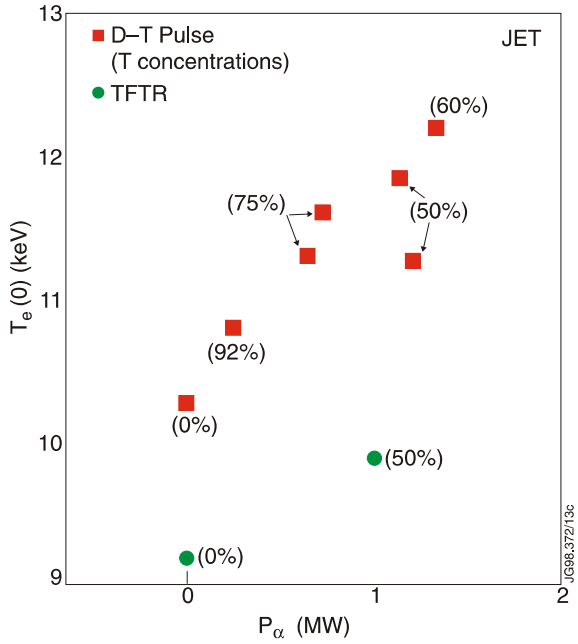

Figure 6: Central electron temperature versus alpha particle power in JET and TFTR DT discharges (adapted from [5], see text for details)

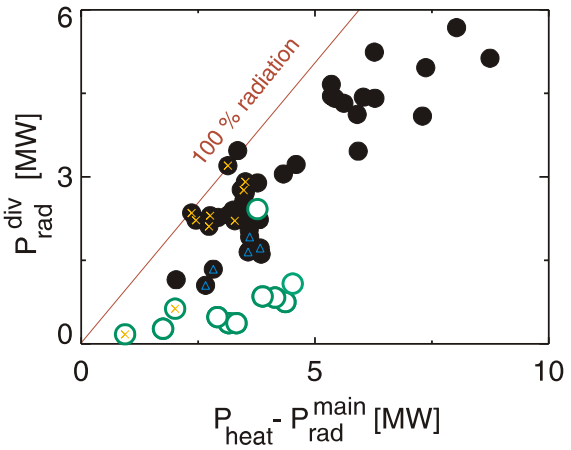

Figure 7: Power radiated in the divertor of ASDEX Upgrade as a function of the power flow into the scrape-off layer in neutral beam heated discharges - Divertor I (open symbols) and Divertor II (Lyra divertor, full symbols) (adapted from [49])

owing to radiation from the plasma center. In this context *all* kind of impurities have to be considered: eroded and injected impurities as well as the helium ash born in the plasma center. The criterion for helium exhaust has been defined by introducing an effective helium exhaust time $\tau^*_{p,He}$. For a steady state burn it has to be at least smaller than 15 energy confinement times τ_E (cf. also [41]). With additional impurities this upper limit becomes smaller. In divertors values for $\rho = \tau^*_{p,He}/\tau_E$ as low as 5 have already been achieved [42].

This burn condition is necessary but not sufficient for steady state operation. The integrity of plasma facing components will crucially depend on the avoidance of overheating of plasma facing components and on the balance between erosion and deposition of wall materials. The lifetime of plasma facing components will ultimately govern the availability of a fusion reactor, an important factor for its economics. The problem of overheating of small areas like the divertor strike zone or the limiter edge can be solved by distributing the power on large areas. In the high density divertor charge-exchange processes could provide this to a certain extent [43]. A distribution of the heat on the whole vessel wall can be achieved by radiation from injected impurities. Feed-back control of the seeded impurities is an important requirement [44]. Up to 90% of the heating power can be radiated from a rather thin belt at the periphery of the confined plasma (cf. also [45]). In the limiter tokamak TEXTOR it was found that the energy confinement with seeded impurities can be substantially improved to values comparable with ELM-free H-mode discharges in divertor tokamaks. This regime has been name *Radiative Improved Mode (RI-mode)* [46]. The RI- mode represents a scenario in which many crucial issues are solved simultaneously: power exhaust to large surfaces, high energy confinement and highest plasma densities. The confinement improvement has been attributed to the suppression of so called ion temperature gradient (ITG) driven modes [47]. However, at reactor relevant collisionalities the impurity content to obtain a confinement transition may be unacceptably high [48].

On ASDEX Upgrade it could be shown that with an appropriate divertor geometry even intrinsic impurities (carbon) can provide a significant radiation level inside the divertor [49]. Fig. 7 shows that the radiation level can reach nearly 100% of the power flowing into the edge plasma with a very closed divertor configuration (Lyra divertor). The rather high level of intrinsic carbon providing this radiation level points to the problem of erosion (predominantly chemical erosion in the Lyra divertor) and deposition. Erosion of graphite is considered to be a severe problem in view of acceptable life times of plasma facing components. On the other hand also areas with significant deposition rates are observed. Thick layers of $100 - 200\mu m$ of carbon deposit are found. These layers may accumulate significant amounts of tritium, which might be unacceptable for reactor operation. Thus, an outstanding issue of research is to control erosion and deposition processes, such that a maximum of eroded material is transported back to its origin where it is re-deposited (see [50]).

Extensive studies have been performed at JET to establish a radiating divertor by using nitrogen [51] [52]. Here it was possible to radiate up to 90% of the heat-

ing power mainly from the divertor. At the high radiation levels, the ELMs are of type- III (see discussion in the next section) and the divertor is detached from the target plates. The heat flux density is reduced to $2MWm^{-2}$ under these conditions. However, the energy confinement time is reduced by about 25% by the degradation of the edge pedestal (see next section).

V. PLASMA EDGE AND GLOBAL CONFINEMENT PROPERTIES

The overall impact of plasma boundary conditions on the general plasma performance and the operational limits of tokamaks has been manifested in many experimental findings. E.g. wall coatings have extended the density domain of tokamak discharges significantly via the reduction of oxygen and material erosion [53]. Furthermore, wall conditioning has turned out to be an important tool to optimise various regimes of improved confinement (limiter conditioning [54]/ Lithium pellets [55] in TFTR in the case of so called "super shots"). Some regimes have been discovered in the course of applying new conditioning schemes (VH- mode in DIII-D after boronization [56]) or active control of plasma edge parameters (RI-mode at TEXTOR with impurity seeding to form a radiating mantle [57]). On the other hand, during experiments to study the issues of power and particle exhaust and the underlying physical processes it has become evident that optimum plasma parameters for exhaust may not be optimum for core confinement (e.g. the influence of impurity seeding and high plasma density by gas fuelling in ELMy H- modes). As a consequence the non-linear interplay between edge and core plasma has been identified as a key issue in present tokamak experiments. The link between plasma edge characteristics and global confinement properties shall now be illustrated using the example of the H-mode.

Evidence for the importance of plasma edge properties was found in the first experiments showing that careful wall conditioning and low recycling are prerequisites to access the H-mode [58]. The build-up of neutral particles has been made responsible for the deterioration of confinement with increased recycling flux [59]. For a long time the conditions to access the H-mode have been described in terms of a threshold power through the separatrix as a function of global discharge parameters. Multi- machine scalings have been made to establish the dependence of the threshold power on the machine size (cf. [60] for a recent scaling). Nevertheless, a significant uncertainty remains, e.g. for the projection of the H-mode threshold power in ITER. As a consequence of improved diagnostics at the plasma edge, it has become possible to describe the operational boundaries for the H-mode in terms of local edge parameters. Fig. 8 shows such an *edge operational diagram* [61]. Shown are the temperature and density on the top of the H-mode pedestal. The simplifying assumptions are made, that the electron temperature and density are comparable to the respective ion features and that the pressure at the top of the pedestal is large compared to the pressure at the separatrix, such that with a fixed width of the pedestal the pressure can be linked to the pressure gradient in the H-mode transport barrier.

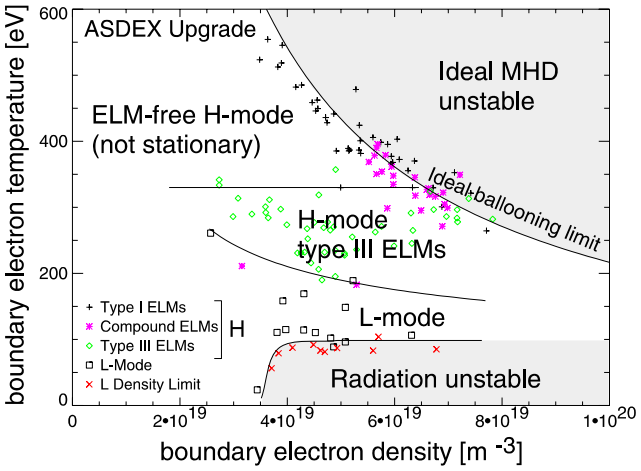

Figure 8: Edge operational diagram of ASDEX-Upgrade (see text for details, adapted from [61])

Different boundaries can be identified in the edge operational diagram. The limit for the pressure gradient building up and leading to type- I ELMs is given by MHD stability and is linked to the onset of coupled ballooning / kink (or peeling) modes (see e.g. [62]). In these models, both the edge pressure gradient and the edge current density is taking into account as causes for MHD instabilities. It is found experimentally that type-I ELMy H-mode discharges are close to this limit with respect to their edge pressure gradient (crosses in Fig. 8). Besides operation at higher plasma currents a further possibility to increase the MHD limits is to shape the plasma towards higher triangularity δ to make the plasma more D- shaped, such that the magnetic field lines stay longer in the "good curvature" region at the high field side where pressure and magnetic field gradients are anti- parallel. As a consequence the critical gradient is substantially increased with δ [63].

This fact is depicted in Fig. 9 [63] where the the edge pressure gradient normalized to the first ballooning stability limit from experiments in DIII-D (using twice the electron pressure) and MHD stability calculations are shown as a function of the averaged triangularity. Note, that at high δ both experiment and modelling show access to the so called "second stability" region [64] which is only possible in non- circular plasmas.

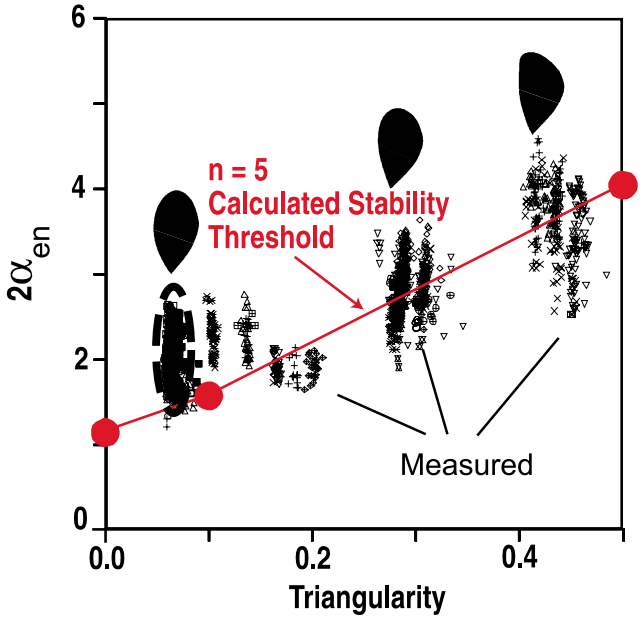

Figure 9: Critical edge pressure gradient vs. averaged triangularity in DIII-D (see text for details, adapted from [63])

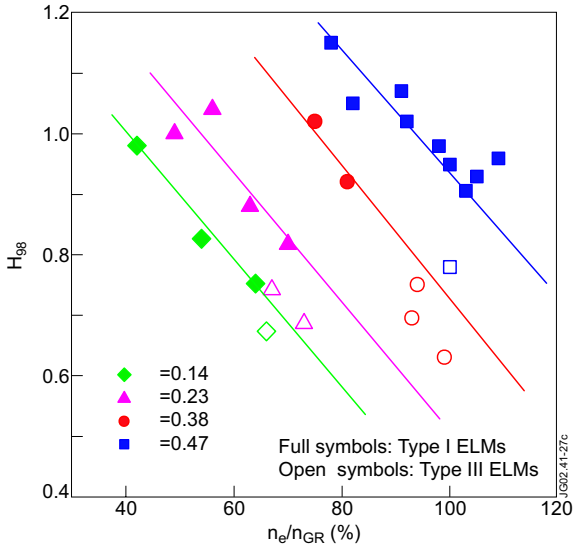

Figure 10: Confinement enhancement factor $H98$ as a function of the plasma line average density n_e, normalized to the Greenwald density, n_{GR} [73].

The second important boundary is the L-H boundary to be crossed to access the H-mode. Experiments on ASDEX-upgrade have indicated a minimum edge temperature needed for the transition from L- to H-mode [61]. Later on, this finding has been confirmed on other devices allowing to establish a multi- machine scaling for the critical temperature [60].

Theoretically the existence of a critical edge temperature has been linked to the existence of a minimum temperature to stabilize drift Alfén waves which are made responsible for anomalous electron transport at the edge [66]. As a consequence of this transport reduction steep gradients of the electron temperature and density develop which in turn lead to increased radial electric fields and sheared ExB rotation. The latter finally stabilizes also ion turbulence, resulting in the formation of the H-mode barrier for electron, ion energy as well as particle transport (cf. discussion in [67]). However, the accuracy of the local edge measurements in the different devices is presently not high enough to rule out the possibility that additional instabilities are important for the L-H transition (cf. [68]).

The boundary between ELM-free H-modes and so called type- III ELMy H-modes is also found to be defined by a characteristic temperature (type- III ELMs are attributed to unstable peeling modes [69] and are characterized by a reduction of the ELM frequency with increasing power through the separatrix, see [70] for a review of ELM characteristics). Finally the last boundary is given by the onset of a thermal instability of the edge plasma, a MARFE [71], leading to a localized radiation and cooling and a disruption of the discharge if the edge temperature is too low.

In the H-mode the height of the edge pedestal determines the global confinement because the edge temperature determines energy transport in the core as the temperature profiles are "stiff", meaning that the core temperature is proportional to the edge pedestal temperature. Such a kind of behavior can be expected if the core transport is characterized by critical temperature gradient lengths [17]. From the viewpoint of power exhaust the operational point desired for the ELMy H-mode is at high densities. However, the rather small gap between the MHD stability limits and the back transition to L-mode makes a careful control of particle fuelling and heating necessary. Generally, it is found that the energy confinement in H-mode discharges significantly deteriorates towards high densities where frequent type- III ELMs prevail. Recent experiments with increased triangularity allowed to improve H-mode confinement for high densities because the stability limits are increased as mentioned above and type- I ELMs can be maintained [72] [73]. This fact is illustrated in Fig. 10 (from [73]), where the energy confinement time normalized to the ELMy H-mode scaling (IPB98(y,2) [2]) is shown as a function of the Greenwald number (the line averaged central density normalized to the current density [74]) for ELMy H-mode discharges at JET with different δ. For a given density, the confinement is clearly improved with increases δ. Nevertheless, still the confinement degrades with increasing density up to the point where the type- I ELMs are replaced by type- III ELMs.

Under certain conditions (mainly at higher safety factor at the edge) interesting regimes with very small ELMs (labelled type- II ELMs) are observed [75] [76] [77] which are attributed to high n MHD modes with a very narrow radial extend [69]. Intense research has started to investigate such kind of scenarios which give prospect for a combination of good energy confinement at high densities with tolerable ELMs. However, extrapolation of these regimes to larger machines remains an issue. Therefore, operational schemes have been sought to actively control the ELMs. Two different approaches are followed.

The first approach aims at controlling the ELM frequency at a level high enough that the edge pedestal cannot increase too much and the ELM crashes are not too large. One possible technique is here the periodic injection of shallow deuterium pellets which had been pioneered in ASDEX Upgrade [78] and developed towards an "integrated exhaust scenario" where "pellet pace making" is combined with a radiating plasma mantle built-up by argon radiation [79]. A second technique is based on periodic vertical plasma movements which trigger ELMs [80] [81].

The second approach to control ELMs is based on ergodization of the magnetic field at the plasma edge. In the DIII-D tokamak it could be shown that by the application of resonant magnetic fields in H-mode plasmas large typ-I ELMs could be completely suppressed [82] [83] [84]. At the same time, the transport barrier at the edge could be maintained as well as the good global energy confinement. An example of such a discharge is illustrated in Fig. 11 together with a reference discharge without edge ergodization. So far, the detailed mechanisms of this very promising technique are not clear, therefore, more insight into the transport in stochastic fusion plasmas is required as well as the application of the technique in further devices, such as JET.

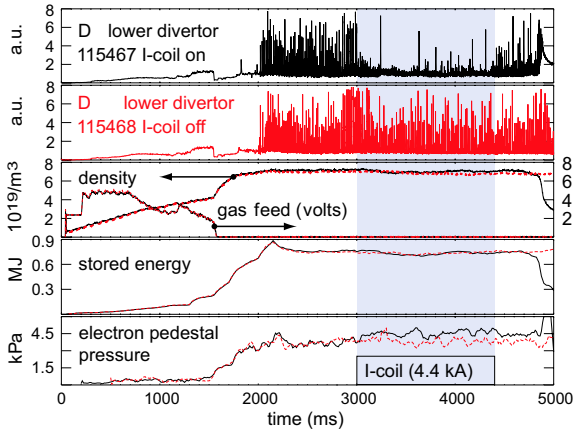

Figure 11: Comparison of ELM suppression and core confinement in identical discharges with (solid lines, shot 115467) and without (dashed lines, shot 115468) an $n = 3$ odd parity $\phi_{tor} = 0^o$ I-coil pulse of $4.4kA$, panels from top to bottom: D_α recycling I-coil on, D_α recycling I-coil off, plasma density and external gas feed, stored energy and electron pressure at the top of the H-mode pedestal (adapted from [84])

.

REFERENCES

1. J.A. Wesson, "Tokamaks", 3rd Edition, Clarendon Press, Oxford (2004).

2. ITER Physics Basis Editors and ITER Physics Expert Groups Chairs and Co- Chairs, Nucl. Fusion **39** (1999), 2137-2664.

3. JET Team, presented by P.H. Rebut, Proc. 13th Int. Conf. on Plasma Physics and Controlled Nuclear Fusion Research, Washington 1990, IAEA-CN-53A-1-2 (1991).

4. T. Fujita and the JT-60 Team, Plasma Phys. Control. Fusion, **39** (1997), B75.

5. J. Jaquinot and the JET team, Plasma Phys. Control. Fusion, **41** (1999), A13.

6. R. Hawryluk, Rev. Mod. Phys **70** (1998), 537.

7. Y. Kusama and the JT-60 team, Phys. of Plasmas **5** (1999), 1935.

8. Y. Shimomura et al., Nucl. Fusion **41** (3) (2001), 309.

9. M. Shimada et al., Nucl. Fusion **44** (2004), 350.

10. J. Cordey et al., Plasma Phys. Control. Fusion **38** (1996) A67.

11. J. Ongena, "Extrapolation to reactors", these proceedings.

12. R. Wolf, Plasma Phys. Control. Fusion **45** (2003), R1.

13. R. Wolf, "A tokamak reactor based on advanced concepts", these proceedings.

14. J.W. Connor et al., Nucl. Fusion **44** (2004) R1.

15. A.C.C. Sips et al., Plasma Phys. Control. Fusion **47** A19.

16. J.W. Connor and H.R. Wilson, Plasma Phys. Control. Fusion **36** (1994), 719.

17. M. Kotschenreuther et al., Phys. Plasmas **2** (1995), 2381.

18. J. Weiland, "Collective Modes in inhomogeneous Plasma", Plasma Physics Series, IoP Publishing Ltd, Bristol, UK (2000).
19. F. Jenko, W. Dorland and G.W. Hammet, Plasma Phys. Plasmas **8** (2001), 4096.
20. J. Candy and R.E. Waltz, Phys. Rev. Lett. **91** (2003), 045001.
21. S. von Goeler, W. Stodiek and N Sauthoff, Phys. Rev. Lett. **33** (1975), 1201.
22. D.W. Faulconer, "Current Drive", these proceedings.
23. F. Wagner et al., Phys. Rev. Lett. **49** (1982), 1408.
24. M. Greenwald et al., Phys. Plasmas **6** (1999), 1943.
25. C.M. Greenfield et al., Phys. Rev. Lett. **86** (2001), 4544.
26. E.A. Lazarus et al., Phys. Rev. Lett. **77** (1996), 2714.
27. C.S. Chang and F.L. Hinton, Phys. Fluids **29** (1986), 3314.
28. O. Sauter et al., Phys. Rev. Lettr. **84** (2000), 3322.
29. K.H. Burrell et al., Phys. Plasmas **8** (2001), 2153.
30. S. Günther et al., Phys. Rev. Lett. **84** (2000), 3097.
31. R. Dux et al., J. Nucl. Mater. **313-316** (2003), 1150.
32. W.P. West et al., Phys. Plasmas **9** (2002) 1970.
33. E. Joffrin et al., Nucl. Fusion **45** (2005), 626.
34. M.R. Wade et al., Nucl. Fusion **45** (2005), 407.
35. A. Staebler et al., Nucl. Fusion **45** (2005), 617.
36. H. Wilson "Neo-classical tearing mode", these proceedings
37. H.P. Furth, R.J. Goldstone, S.J. Zweben and D.J. Sigmar, Nucl. Fusion **30** (1990), 1799.
38. W.W. Heidbrink and G.J. Sadler, Nucl. Fusion **34** (1994), 535.
39. T.H. Stix, Plasma Phys. **14** (1972), 367.
40. S.J. Zweben et al., Plasma Phys. Control. Fusion **39** (1997), A275.
41. D. Reiter, "Recycling and transport of neutrals", these proceedings.
42. H.S. Bosch et al., J. Nucl. Mater. **266-269** (1999), 462.
43. M.L. Watkins and P.H. Rebut, Europhys. Conf. Abstracts (Proc. 19th Europ. Conf. Controlled Fusion and Plasma Physics, Insbruck 1992) Vol. II p. 731.
44. U. Samm et al., Plasma Phys. Control. Fusion **35** (1993), B167.
45. B. Unterberg, "Overview of plasma edge physics", these proceedings.
46. A.M. Messiaen et al., Phys. Rev. Lettr. **77** (1996), 2487.
47. M.Z. Tokar' et al., Plasma Phys. Control. Fusion **41** (1999), L9.
48. M.Z. Tokar' et al., Plasma Phys. Control. Fusion **44** (2002), 1903.
49. A. Kallenbach et al, Plasma Phys. Control. Fusion **41** (1999), B177.
50. U., Samm, "Plasma wall interaction", these proceedings.
51. J. Rapp et al., Plasma Phys. Control. Fusion **44** (2002), 639.
52. J. Rapp et al., Nucl. Fusion **44** (2004), 312.
53. H.R. Koslowski, "Operational limites in tokamak machines and limiting instabilities", these proceedings.
54. J.D. Strachan et al., Phys. Rev. Lett. **58** (1987), 1004.
55. J.L. Terry et al., Nucl. Fusion (Suppl. 1) (1991), 393.
56. G.L. Jackson et al., Phys. Rev. Lett. **67** (1991), 3089.
57. B. Unterberg et al., Plasma Phys. Control. Fusion **39** (1997), B189.
58. ASDEX team, Nucl. Fusion **29**(1989), 1959.
59. S. Senguku et al, J. Nucl. Mater. **176-177**(1990), 65.
60. J.A. Snipes and the International H-mode Threshold Database Working Group, Plasma Phys. Control. Fusion **42** (2000), A299.

61. W. Suttrop et al., Plasma Phys. Control. Fusion **39** (1997), 2051.

62. J.W. Conner et al., Phys. Plasmas **5** (1998), 2687.

63. L.L. Lao et al., Nucl. Fusion **41** (2001), 295.

64. J.M. Greene and M.S. Chance, Nucl. Fusion **21** (1981), 453.

65. T.N. Carlstrom et al., Nucl. Fusion **39** (1999), 1941.

66. O. Pogutse et al., 24th European Physical Society Conference Controlled Fusion and Plasma Physics (Berchtesgaden 1997), Europ. Conference Abstracts, Vol 21A, part III, 1041.

67. Yu. Igitkhanov, Plasma Phys. Control. Fusion **40** (1998), 837.

68. J.W. Connor and H.R. Wilson, Plasma Phys. Control. Fusion **42** (2000), R1.

69. W. Suttrop et al., Plasma Phys. Control. Fusion **42** (2000), A1.

70. H. Zohm, Plasma Phys. Control. Fusion **48** (1996), 105.

71. B. Lipschultz et al., Nucl. Fusion **24** (1984), 977.

72. J. Stober et al., Plasma Phys. Control. Fusion **42** (2000), A211.

73. G. Saibene et al., Plasma Phys. Control. Fusion **44** (2002), 1769.

74. M. Greenwald et al., Nucl. Fusion **28** (1988), 2199.

75. DIII-D Team, Proc. 13th Int. Conf. on Plasma Physics and Controlled Nuclear Fusion Research, Washington 1990, IAEA-CN-53/A-I-4 (1991)

76. J. Stober et al., Nucl. Fusion **41** (2001), 1123.

77. Y. Kamada et al., Plasma Phys. Control. Fusion **42** (2000), A247.

78. P.T. Lang et al., Nucl. Fusion **44** (2004), 665.

79. P.T. Lang et al., Nucl. Fusion **45** (2005), 502.

80. A.W. Degeling et al., Plasma Control. Fusion **45** (2003) 1637.

81. P.T. Lang et al., Plasma Phys. Control. Fusion **46** (2004), L31.

82. T.E. Evans et al., Phys. Rev. Lett. **92**, 23503 (2004)

83. T.E. Evans et al., Nucl. Fusion **45** (2005), 595.

84. R.A. Moyer et al., Phys. Plasmas **12**, 056119 (2005)